Skeletal muscle fiber-type switching, exercise intolerance, and myopathy in PGC-1alpha muscle-specific knock-out animals.

Handschin, Christoph ; Chin, Sherry ; Li, Ping ; Liu, Fenfen ; Maratos-Flier, Eleftheria ; Lebrasseur, Nathan K ; Yan, Zhen ; Spiegelman, Bruce M

Abstract: The transcriptional coactivator peroxisome proliferator-activated receptor gamma coactivator 1alpha (PGC-1alpha) is a key integrator of neuromuscular activity in skeletal muscle. Ectopic expression of PGC-1alpha in muscle results in increased mitochondrial number and function as well as an increase in oxidative, fatigue-resistant muscle fibers. Whole body PGC-1alpha knock-out mice have a very complex phenotype but do not have a marked skeletal muscle phenotype. We thus analyzed skeletal muscle-specific PGC-1alpha knock-out mice to identify a specific role for PGC-1alpha in skeletal muscle function. These mice exhibit a shift from oxidative type I and IIa toward type IIx and IIb muscle fibers. Moreover, skeletal muscle-specific PGC-1alpha knock-out animals have reduced endurance capacity and exhibit fiber damage and elevated markers of inflammation following treadmill running. Our data demonstrate a critical role for PGC-1alpha in maintenance of normal fiber type composition and of muscle fiber integrity following exertion.

DOI: https://doi.org/10.1074/jbc.M704817200

THE JOURNAL OF BIOLOGICAL CHEMISTRY VOL. 282, NO. 41, pp. 30014–30021, October 12, 2007

Skeletal Muscle Fiber-type Switching, Exercise Intolerance, and Myopathy in PGC-1α Muscle-specific Knock-out Animals*[S]

Received for publication, June 12, 2007, and in revised form, July 5, 2007 Published, JBC Papers in Press, August 16, 2007, DOI 10.1074/jbc.M704817200

Christoph Handschin[‡§1], Sherry Chin[‡], Ping Li[¶], Fenfen Liu[‖], Eleftheria Maratos-Flier[‖], Nathan K. LeBrasseur[**], Zhen Yan[¶], and Bruce M. Spiegelman[‡2]

From the [‡]Dana-Farber Cancer Institute and Department of Cell Biology, Harvard Medical School, Boston, Massachusetts 02115, [§]Institute of Physiology and Zurich Center for Integrative Human Physiology, University of Zurich, Winterthurerstrasse 190, CH-8057 Zurich, Switzerland, [¶]Department of Medicine, Duke University Medical Center, Durham, North Carolina 27704, [‖]Division of Endocrinology, Diabetes, and Metabolism, Department of Medicine, Beth Israel Deaconess Medical Center and Harvard Medical School, Boston, Massachusetts 02215, and [**]Diabetes and Metabolism Unit, Boston University School of Medicine, Boston, Massachusetts 02118

The transcriptional coactivator peroxisome proliferator-activated receptor γ coactivator 1α (PGC-1α) is a key integrator of neuromuscular activity in skeletal muscle. Ectopic expression of PGC-1α in muscle results in increased mitochondrial number and function as well as an increase in oxidative, fatigue-resistant muscle fibers. Whole body PGC-1α knock-out mice have a very complex phenotype but do not have a marked skeletal muscle phenotype. We thus analyzed skeletal muscle-specific PGC-1α knock-out mice to identify a specific role for PGC-1α in skeletal muscle function. These mice exhibit a shift from oxidative type I and IIa toward type IIx and IIb muscle fibers. Moreover, skeletal muscle-specific PGC-1α knock-out animals have reduced endurance capacity and exhibit fiber damage and elevated markers of inflammation following treadmill running. Our data demonstrate a critical role for PGC-1α in maintenance of normal fiber type composition and of muscle fiber integrity following exertion.

Skeletal muscle has an enormous capacity to adapt to motor neuron activity. Many changes in gene expression are controlled by motor neuron-induced calcium signaling (1–3). The transcriptional coactivator peroxisome proliferator-activated receptor γ coactivator 1α (PGC-1α)[3] is at the nexus of this signaling and subsequently regulates the expression of gene programs needed for skeletal muscle adaptations to increased work load (4, 5). By coactivating the myocyte enhancer factor 2 members MEF2C and MEF2D, PGC-1α potently drives transcription of myofibrillar genes typical of oxidative muscle fibers (6). Interestingly, MEF2 and PGC-1α also control PGC-1α gene transcription in an autoregulatory loop (7, 8). Metabolic genes, including those responsible for mitochondrial oxidative phosphorylation, are induced by a transcriptional cascade with coactivation of the estrogen-related receptor α (ERRα, official nomenclature NR3B1), the nuclear respiratory factor 2 (NRF-2, alternatively called GA-binding protein, GABP), and the nuclear respiratory factor 1 (NRF-1) by PGC-1α and subsequent increase in the levels of mitochondrial transcription factor A (TFAM) and mitochondrial transcription specificity factors TFB1M and TFB2M (9–13). Recently, we have found that activity-induced remodeling of the postsynaptic side of neuromuscular junctions involves a complex between PGC-1α, GABP, and host cell factor that assembles upon phosphorylation of PGC-1α and GABP in post-synaptic nuclei (14).

Data obtained from muscle-specific PGC-1α transgenic animals underline the importance of PGC-1α in skeletal muscle *in vivo* (6). These mice have increased number and function of mitochondria accompanied by a higher number of type IIa and type I oxidative, slow twitch, high endurance muscle fibers (6). Furthermore, even in the absence of functional motor nerve signaling following hind leg denervation, ectopically expressed PGC-1α maintains skeletal muscle function and blunts skeletal muscle atrophy that normally occurs in the absence of motor neuron signaling (15). Thus, PGC-1α apparently controls most if not all of the transcriptional changes induced by motor neuron signaling in skeletal muscle. Surprisingly, whole body PGC-1α knock-out animals do not exhibit a marked skeletal muscle phenotype (16). Despite a significant reduction of transcription of several mitochondrial genes, no difference in the relative numbers of the different fiber types is observed (17). However, whole body PGC-1α knock-out animals have a dominant central nervous system phenotype that might mask the effects of loss-of-function of PGC-1α in peripheral tissues (16). These mice are hyperactive, show circadian abnormalities, and have constitutively activated AMP-activated kinase in skeletal muscle, all of which might compensate for the loss of PGC-1α in this tissue (16, 18). In the liver, gluconeogenic and heme biosynthetic genes are constitutively elevated in whole body PGC-1α knock-out animals even in the fed state (16). In contrast, and as expected from previous studies, fasting induction

* This work was supported in part by National Institutes of Health Grants DK54477 and DK61562 (to B. M. S.) and AR050429 (to Z. Y.). The costs of publication of this article were defrayed in part by the payment of page charges. This article must therefore be hereby marked "*advertisement*" in accordance with 18 U.S.C. Section 1734 solely to indicate this fact.

[S] The on-line version of this article (available at http://www.jbc.org) contains supplemental Figs. S1–S4.

[1] Supported by a Scientist Career Development grant from the Muscular Dystrophy Association, Swiss National Science Foundation Professorship PP00A-110746, and the University Research Priority Program "Integrative Human Physiology" of the University of Zurich.

[2] To whom correspondence should be addressed: Dana-Farber Cancer Institute, Smith Bldg., One Jimmy Fund Way, Boston, MA 02115. Tel.: 617-632-3567; Fax: 617-632-4655; E-mail: bruce_spiegelman@dfci.harvard.edu.

[3] The abbreviations used are: PGC-1α, peroxisome proliferator-activated receptor γ coactivator 1α; MKO, skeletal muscle-specific knock-out animals; MyHC, myosin heavy chain; TNFα, tumor necrosis factor α.

of gluconeogenic and heme biosynthetic genes is severely blunted in the liver of liver-specific PGC-1α knock-out animals (19).

To clarify the genetic requirement for PGC-1α in skeletal muscle function without the confounding variables seen in the whole body knockouts, skeletal muscle-specific PGC-1α knock-out animals (MKOs) were generated.[4] Here, we report a moderate reduction in the number of oxidative type I and type IIa muscle fibers and exercise capacity in these mice. Strikingly, skeletal muscle of MKOs has a low level of damaged and regenerating fibers. This compromised skeletal muscle integrity is dramatically exacerbated by physical exercise and accompanied by elevated markers of systemic inflammation. Our data thus highlight the importance of PGC-1α in maintaining proper function and integrity of skeletal muscle.

EXPERIMENTAL PROCEDURES

Animal Experimentation—Generation of MKOs has been described elsewhere.[4] Mice were held under standard conditions. All experiments and protocols were performed in accordance with the respective Animal Facility Institutional Animal Care and Use Committee regulations.

Gene Expression Analysis—Total RNA was isolated from tissues using the TRIzol reagent (Invitrogen) according to the manufacturer's instructions. After DNase I digest, 1 μg of total RNA was reverse transcribed and analyzed using Applied Biosystems Real-time PCR System 7300 using the ΔΔCt method. Relative gene expression was normalized to 18 S rRNA levels.

Histology—Tissues were dissected, embedded in OCT compound (VWR Scientific), dehydrated, embedded in paraffin, and sectioned. The sections were subsequently stained with hematoxylin and eosin. Evans blue dye (1% solution) was intraperitoneal injected at a concentration of 1% volume/bodyweight 16 h before the treadmill exercise. Mice were sacrificed pre- and 30 min post-exercise and skeletal muscle frozen histological sections prepared. Evans blue incorporation was analyzed by fluorescence microscopy. Evans blue-penetrated muscle fibers and fibers with centrally located nuclei were counted in 20 randomly chosen sections in blinded fashion and were normalized by the total number of muscle fibers per field. Immunofluorescent staining for type I, type Iia, and type IIb muscle fibers was performed with antibodies against the respective myosin heavy chains as described (20). The relative numbers of the different fiber types were quantified by counting 20 sections of each muscle bed (type I, red; type Iia, blue; type Iix, black; type Iib, green).

Comprehensive Laboratory Animal Monitoring System—Comprehensive laboratory animal monitoring system (Columbia Instruments) analysis was performed for four light and three dark periods after an acclimatization of 2 days. Data about locomotive activity were collected every 48 min on 16 mice simultaneously.

Grip Strength—Grip strength was assessed by an inverted screen test as described (21). Each mouse was placed on top of an elevated wire mesh grid, the screen was inverted, and the animals were timed until release from the grid. A maximum score of 60 s was given if the animal did not fall.

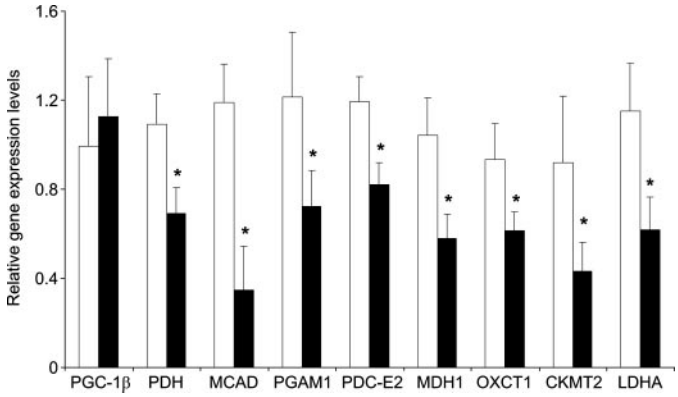

FIGURE 1. **Decreased metabolic gene expression in MKOs.** Relative gene expression was measured from cDNA extracted from gastrocnemius and normalized to 18 S rRNA levels. *Bars* depict mean values, and *error bars* represent standard error. *, $p < 0.05$ between control and MKO animals. *PDH*, pyruvate dehydrogenase β; *MCAD*, medium chain acyl-CoA dehydrogenase; *PGAM1*, phosphoglycerate mutase 1; *PDC-E2*, pyruvate dehydrogenase complex, E2 component; *MDH1*, malate dehydrogenase 1, NAD (soluble); *OXCT1*, 3-oxoacid CoA transferase; *CKMT2*, creatine kinase, mitochondrial 2 (sarcomeric); *LDHA*, lactate dehydrogenase A.

Treadmill Exercise—For 3 days, animals were acclimatized to treadmill running (Columbus Instruments) for 5 min at a speed of 10 m/min and on a 0% grade. One day before the treadmill experiment, animals were injected with a 1% Evans blue dye solution. The next day, animals ran on a treadmill tilted 10% uphill starting at a speed of 10 m/min for 5 min. Every subsequent 2 min, the speed was increased by 2 m/min until mice were exhausted or a maximal speed of 46 m/min was reached (supplemental Fig. S1). Exhaustion was defined as the inability of the animal to remain on the treadmill despite an air puff stimulus and mechanical prodding. Running time was measured and running distance, work, and power calculated. Distance is a function of time and speed of the treadmill. Work is calculated as the product of bodyweight (kg), gravity (9.81 m/s^2), vertical speed (m/s * angle), and time (s). Power is the product of bodyweight (kg), gravity (9.81 m/s^2), and vertical speed (m/s * angle).

Determination of TNFα Serum Concentration—Serum tumor necrosis factor α (TNFα) was determined from mouse serum using a Quantikine Mouse TNFα enzyme-linked immunosorbent assay kit according to the manufacturer's instructions (R&D Systems).

Serum Creatine Kinase Assay—Mouse blood was collected and serum isolated using heparin-coated collection tubes (BD Biosciences). Serum creatine kinase activity was then determined with the Creatine Kinase-SL Assay kit according to the manufacturer's protocol (Diagnostic Chemicals Limited).

Denervation, Determination of Muscle Mass—Disuse atrophy was induced by surgical ablation of the sciatic nerve on one hind leg as described (15). Muscle mass of the control leg and the denervated leg was determined 12 days after the surgery.

Statistical Analysis—All results are expressed as means, and error bars depict standard errors. Two-tailed Student's *t* test was used to determine *p* values. Statistical significance was defined as $p < 0.05$. For all experiments, at least 8 mice/group were used.

[4] Handschin, C., Choi, C. S., Chin, S., Kim, S., Kawamori, D., Kurpad, A. J., Neubauer, N., Hu, J., Mootha, V. K., Kim, Y.-B., Kulkarni, R. N., Shulman, G. I., and Spiegelman, B. M. (2007) *J. Clin. Investig.* in press.

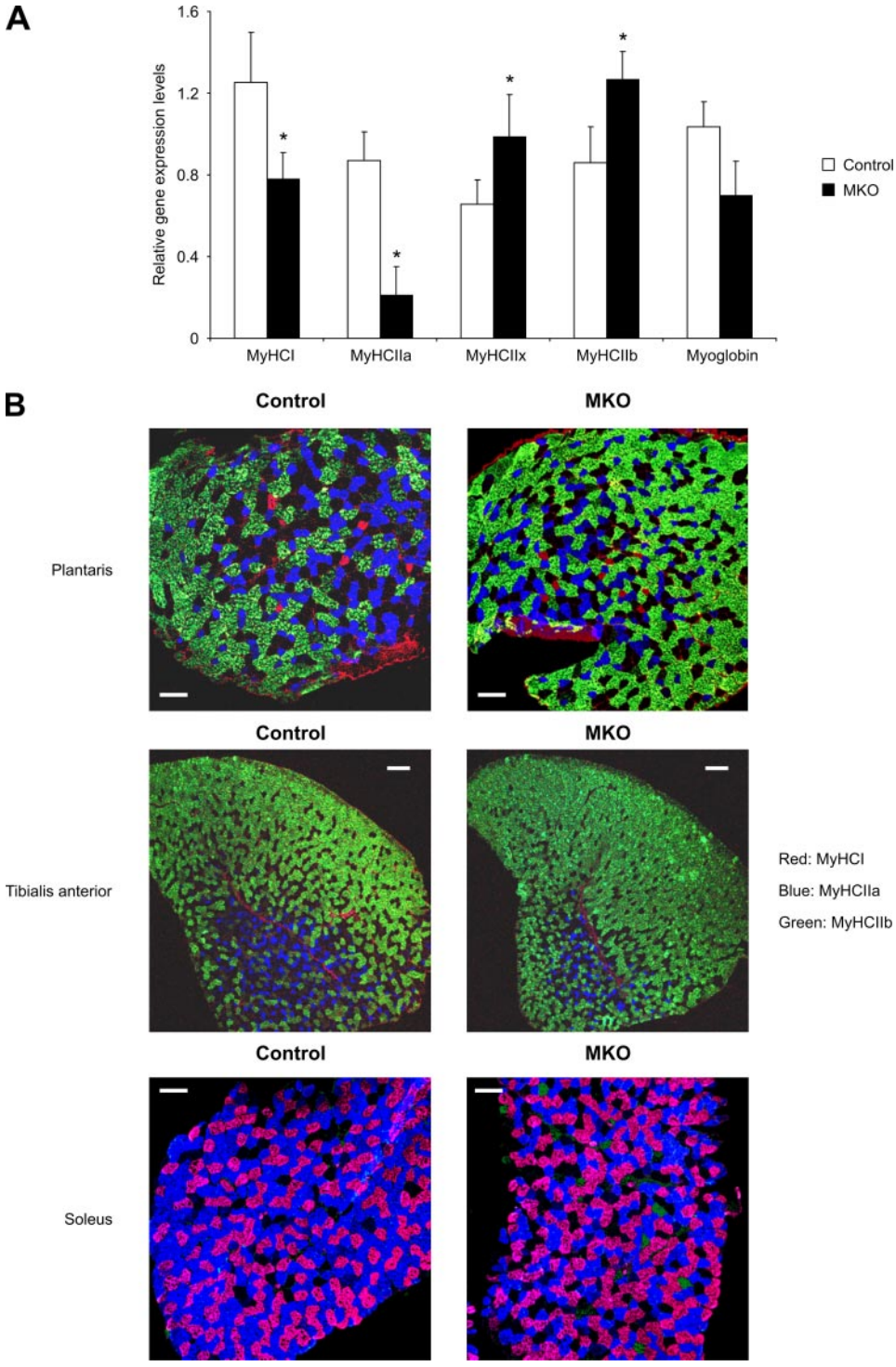

FIGURE 2. **Fiber-type switching toward increased numbers of glycolytic fibers in MKOs.** *A*, relative gene expression was measured from cDNA extracted from gastrocnemius and normalized to 18 S rRNA levels. *B*, cross-sections of plantaris, tibialis anterior, and soleus were immunostained for myosin heavy chains I (*red*), IIa (*blue*), and IIb (*green*). *Bars* depict mean values, and *error bars* represent standard error. *, $p < 0.05$ between control and MKO animals.

RESULTS

Muscle-specific Knock-out Animals of PGC-1α Have an Increased Number of Glycolytic Myofibers—The generation of the MKOs of PGC-1α and analysis of mRNA and protein expression have been described elsewhere.[4] These animals have a reduced expression of number of mitochondrial genes (Fig. 1) that were previously found to be elevated in PGC-1α muscle transgenic mice (15). Interestingly, PGC-1β levels are not altered by PGC-1α ablation in skeletal muscle as a compensatory mechanism (Fig. 1). Mitochondrial gene expression and oxidative metabolism are hallmarks of the slow twitch, oxidative type I and IIa myofiber (3). Thus, to study whether the corresponding myofibrillar gene expression is also altered in MKOs compared with controls, we measured the relative gene expression levels of the respective myosin heavy chain (MyHC) isoforms I, IIa, IIx, and IIb in gastrocnemius by semiquantitative real-time PCR, comparing control to MKO mice. Transcript levels for MyHCI and MyHCIIa were lower in MKOs *versus* control animals, being reduced by 47 and 78%, respectively (Fig. 2*A*). In contrast, MKOs had significantly higher expression of MyHCIIx (+22% *versus* controls) and MyHCIIb (+29% *versus* controls) (Fig. 2*A*), indicating a reduction in oxidative, high endurance fibers and an increase in fast twitch, glycolytic fibers in MKOs. These findings were consistent with histological analysis of different muscle beds (Fig. 2*B* and supplemental Fig. S1). Type IIa fibers were predominantly replaced by type IIb fibers in gastrocnemius, plantaris, and tibialis anterior. In MKO soleus muscle, a muscle rich in type I and IIa fibers, type I and type IIa fibers were reduced by 11 and 45%, respectively, and a clear increase in type IIb fibers was observed (+10%) (Fig. 2*B* and supplemental Fig. S1). In control animals, type IIb fibers were very rarely found in soleus (Fig. 2*B*). Thus, both in terms of gene expression and histology of myofibrillar proteins, skeletal muscles of MKOs have a higher percentage of the glycolytic IIx and IIb fibers at the apparent expense of a loss of oxidative type I and IIa fibers (Fig. 2 and supplemental Fig. S1). Notably, the loss in type IIa fibers exceeds the reduction in type I fibers. In fact, a significant reduction of type I fibers was only observed in the gastrocnemius and the soleus, whereas the number of type IIa fibers was lower in all four muscles. Interestingly, muscle-specific PGC-1α transgenic animals show a

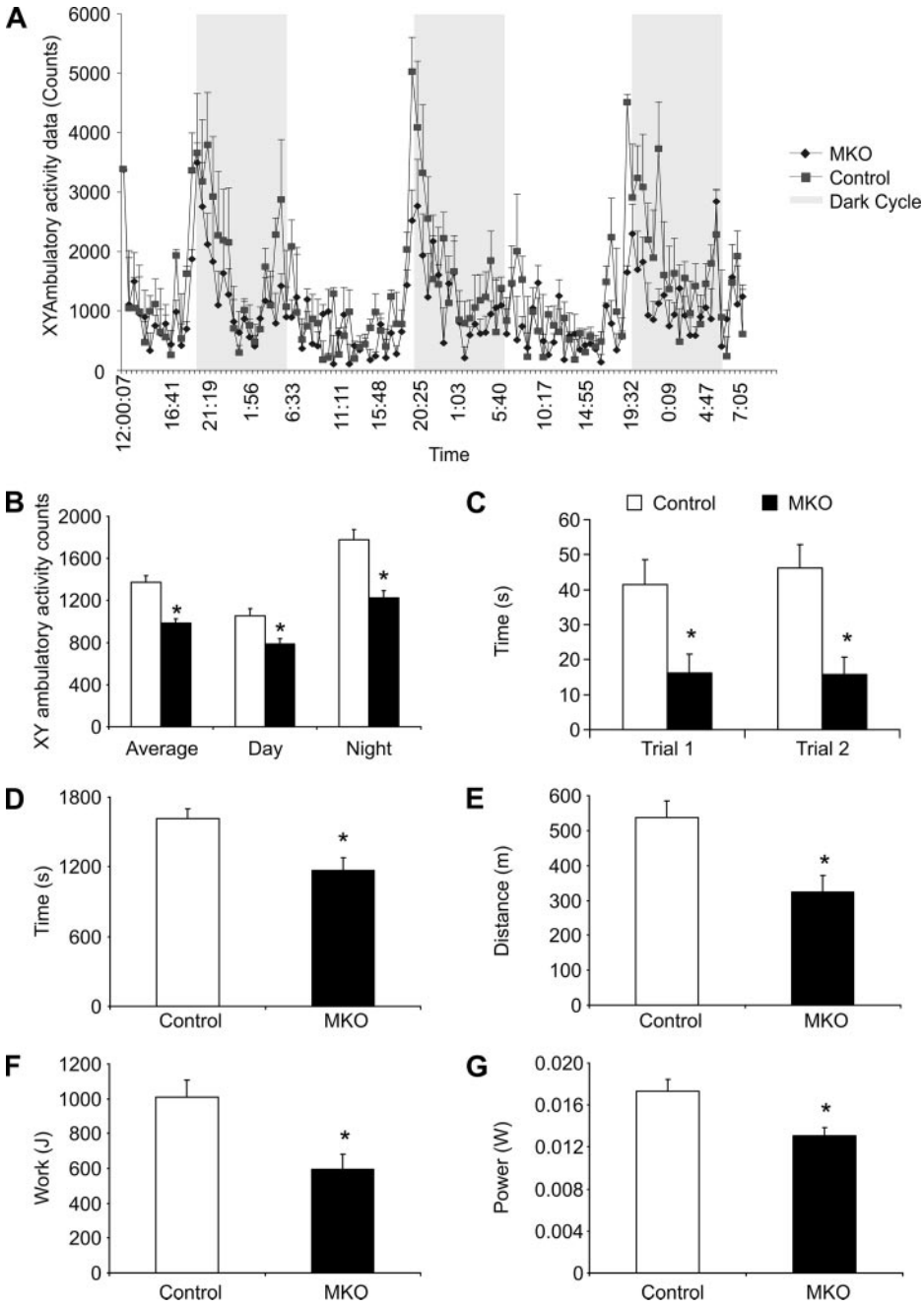

FIGURE 3. **Decreased physical activity and impaired muscle function in MKOs.** *A*, circadian patterns of voluntary locomotive activity were recorded for four light and three dark periods in comprehensive laboratory animal monitoring systems by infrared beam breaking. *B*, average locomotive activity of control mice and MKOs. *C*, grip strength tests assessed the ability of control and MKO animals to hold onto an inverted grid wire mesh. A maximal score of 60 s was assigned to mice that did not fall down. Trial 2 was repeated 30 min after Trial 1. *D–G*, treadmill exercise. After acclimatization, mice were run on a treadmill with a 10% slope and increasing speed to exhaustion. Time (*D*), distance (*E*), work (*F*), and power (*G*) were calculated from the individual performances. *Bars* depict mean values, and *error bars* represent standard error. *, $p < 0.05$ between control and MKO animals.

greater increase in type IIa than type I fibers (6), thus providing a mirror image of the data obtained in MKOs.

Reduced Muscle Function and Exercise Capacity in MKOs—Ectopic expression of PGC-1α in skeletal muscle resulted in a higher fatigue resistance *ex vivo* in isolated muscle fibers (6). Accordingly, PGC-1α levels in muscle correlate with the degree of physical activity: PGC-1α transcription is induced by exercise and repressed by disuse (15, 22). To study the impact of PGC-1α ablation on skeletal muscle function in intact animals, we assessed the physical condition of MKOs and control animals. Monitoring of locomotive activity in comprehensive laboratory animal monitoring systems revealed that MKOs have regular circadian rhythms in terms of physical activity (Fig. 3*A*). However, MKOs are hypoactive compared with control mice (Fig. 3, *A* and *B*). These findings are in stark contrast to the hyperactive PGC-1α total knock-out animals (16). Interestingly, the decrease in physical activity in MKOs is similar in the light and the dark period (Fig. 3*B*). The hyperactivity of PGC-1α total knock-out mice was predominantly caused by abnormal activity during the light period (16). Thus, voluntary physical activity is uniformly reduced in the light and dark phases in MKO mice.

In addition to spontaneous muscle usage, we challenged control and MKO animals with involuntary physical exercise testing muscle endurance. First, muscle grip strength was tested using an inverted screen. Inverted screen tests for muscle grip strength predominantly measure isometric muscle endurance. Previous analyses showed a decreased performance of global PGC-1α knock-out mice in this type of test (21). But because of the various abnormalities in global PGC-1α knockouts, we decided to reassess this in the MKOs. MKO mice showed compromised muscle function compared with the control mice in this assay (Fig. 3*C*). In the two trials, MKOs were able to hold on for an average of 17 and 16 s, respectively, whereas control mice dropped after 42 and 45 s, respectively (Fig. 3*C*). Thus, lack of skeletal muscle PGC-1α leads to a 60% reduction in grip strength performance in MKOs. Previously published results of PGC-1α total knock-out animals in the inverted screen test (21) can now be conclusively explained by impaired muscle function.

Muscle endurance with dynamic fiber contractions was assessed by treadmill running to exhaustion, as an indicator of maximal muscle capacity. After acclimatization, mice were run

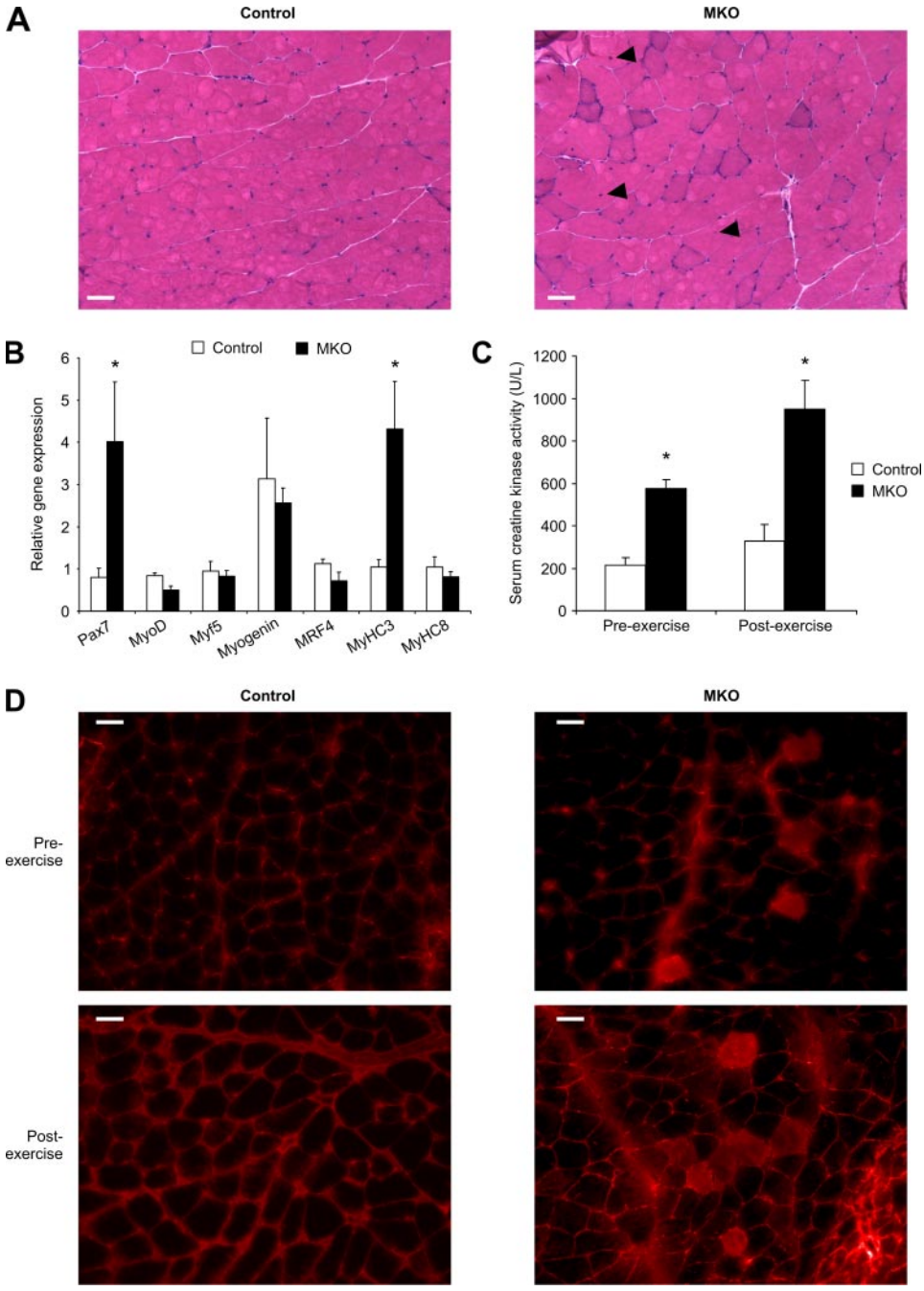

FIGURE 4. **MKOs have damaged muscle fibers.** *A*, hematoxylin and eosin staining of gastrocnemius cross-sections. *Arrowheads* point to muscle fibers with centrally located nuclei. *B*, relative gene expression measured from cDNA of gastrocnemius muscle and normalized to 18 S rRNA levels. *Pax7*, paired box gene 7; *MyoD*, myogenic differentiation antigen 1; *Myf5*, myogenic factor 5; *MRF4*, muscle regulator factor 4; *MyHC*, myosin heavy chain. *C*, serum creatine kinase levels. Serum creatine kinase activity was determined in sedentary animals (pre-exercise) and mice that were sacked 30 min after the treadmill exercise (post-exercise). *D*, Evans blue dye was intraperitoneal injected and mice sacked 16 h later. Post-exercise animals were analyzed 30 min after completion of the treadmill running. *Bars* depict mean values, and *error bars* represent standard error. *, $p < 0.05$ between control and MKO animals.

on a 10% slope with a protocol using increasing speed (supplemental Fig. S2) until the animals were unable to remain on the treadmill despite air puff stimuli and prodding. Control animals ran roughly 7.5 min (28%) longer than MKOs, an average of 26 min and 52 s for the controls *versus* 19 min and 25 s for the MKOs (Fig. 3*D*). The difference in running distance was even bigger because of the running protocol with increasing speed (Fig. 3*E*). Whereas MKOs covered an average distance of 323 meters, control mice ran 536 meters on the average (a difference of 40%). Finally, work and power generated by control animals were also higher than those of MKOs (Fig. 3, *F* and *G*). Control mice used energy equivalent to 1007 J whereas the average work of MKOs came to 594 J (a difference of 41%). Finally, the 17.3 milliwatts of power of the control mice are 25% higher than the 13.1 milliwatts of the MKOs. In summary, all the parameters obtained from the treadmill running experiment describing muscle endurance were significantly lower for MKOs compared with control mice. Thus, the decrease in muscle function in MKOs could consistently be shown in different tests assessing voluntary physical activity and isometric and dynamic muscle endurance. Interestingly, PGC-1α total knock-out animals performed even worse than MKOs in treadmill running (21). This might reflect additional defects in heart function and the motor neuron system in whole body PGC-1α knock-out mice that also contribute to physical endurance.

Basal and Exercise-induced Myopathy in MKOs—Muscle contraction exerts mechanical stress on muscle fibers. Excess stress can lead to muscle damage that is normally offset by muscle regeneration. As described above, MKOs have a diminished capacity for physical movement, both voluntary and forced. In hematoxylin and eosin staining of cross-sections of quadriceps, a higher number of muscle fibers with centrally located nuclei, a hallmark of regenerating muscle fibers, is found in MKOs compared with control mice (Fig. 4*A*). We thus checked the expression of various markers of muscle damage and regeneration to study the impact of muscle-specific PGC-1α ablation on muscle fiber integrity. Interestingly, we observed a massive induction of Pax7 gene expression in MKOs (Fig. 4*B*), a molecular marker for satellite cells (23). In the MKOs, myogenin expression was not significantly decreased. Future studies will address this discrepancy between the published reciprocal regula-

tion between Pax7 and the other muscle regulatory factors in cell culture (24) and our data *in vivo*. In addition to Pax7, transcript levels of MyHC3, normally only observed in embryonic stages of muscle development, were elevated in MKOs compared with control animals (Fig. 4*B*). Together, these data suggest that muscle fiber regeneration is induced in MKOs by increased recruitment of satellite cells and the transient expression of MyHC3 in newly formed muscle fibers. Elevated markers for cell proliferation and decreased levels of genes involved in growth arrest support this hypothesis (supplemental Fig. S3). Increased muscle fiber regeneration is often a sign of muscle damage in mice, and muscle damage leads to higher serum creatine kinase levels in the blood leaking from muscle fibers. We therefore measured serum creatine kinase activity in pre- and post-exercise control and MKO animals, respectively. We found a 3-fold increase in serum creatine kinase in sedentary MKOs compared with controls (Fig. 4*C*). Creatine kinase levels were further elevated by exercise in MKOs (Fig. 4*C*). To estimate the degree of muscle damage in MKOs, we intraperitoneal injected Evans blue dye into control and MKO animals pre- and post-exercise. Evans blue can penetrate damaged muscle fibers and is visualized by fluorescent microscopy of histological sections (*e.g.* see Ref. 14). The increased staining of muscle fibers in pre-exercise MKOs *versus* control animals (Fig. 4*D*) indicated that MKOs exhibit low grade muscle damage, even in the basal state. The number of Evans blue-positive muscle fibers was clearly increased in MKOs post-exercise (Fig. 4*D*). In comparison, control animals have no visible muscle fiber damage after treadmill running (Fig. 4*D*). Thus, skeletal muscle PGC-1α is required in maintaining muscle fiber integrity in the sedentary state; this is even more so during and following physical exertion.

Increased Inflammatory Response in Sedentary and Exercised MKOs—Many different mechanisms could be involved in the muscle damage observed in MKOs. Idiopathic inflammatory myopathies are well described disease pathologies in human patients, and TNFα has been causally implicated in this process (25). We previously noted increased expression of different inflammatory markers in MKO skeletal muscle in a non-exercised state, including elevated mRNA levels for interleukin 6 and TNFα.[4] In addition, circulating interleukin 6 levels in the blood were elevated in MKOs compared with controls, but we did not see a significant difference in circulating TNFα levels in the non-exercised context. To investigate whether elevation of TNFα could be involved in the increase in muscle damage post-exercise, we measured gene expression levels and circulating concentrations of TNFα in mice after treadmill running. In MKOs, TNFα gene expression was higher both pre- and post-exercise compared with control mice[4] (Fig. 5*A*). Remarkably, transcript levels of TNFα were massively increased in exercised MKOs compared with pre-exercised MKOs, whereas no change in TNFα expression was observed in control mice before and after physical activity (Fig. 5*A*). This increase in gene expression was paralleled by a marked rise in circulating TNFα in the blood of MKOs (Fig. 5*B*). In fact, in sedentary MKOs and sedentary or exercised control animals, circulating TNFα

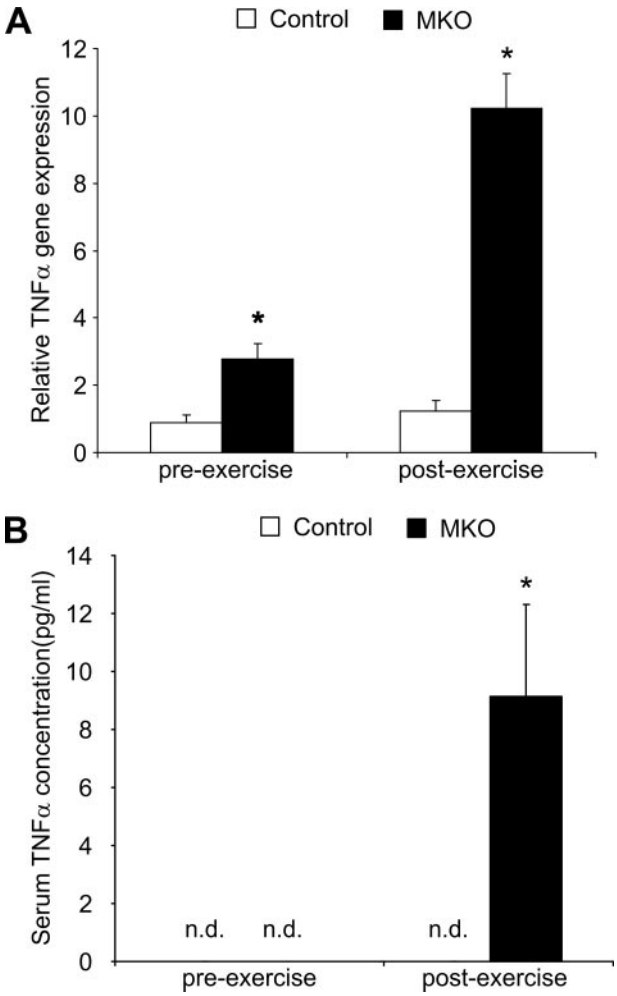

FIGURE 5. **Increased expression of TNFα in MKO skeletal muscle.** *A*, relative gene expression of TNFα normalized to 18 S rRNA levels in control and MKO animals that were sedentary (pre-exercise) or exercised (post-exercise), respectively. *B*, circulating TNFα concentration in control and MKO animals that were sedentary (pre-exercise) or exercised (post-exercise), respectively. *n.d.*, not detectable. *Bars* depict mean values, and *error bars* represent standard error. *, $p < 0.05$ between control and MKO animals.

levels were below the detection limit of our assay and we could only detect circulating TNFα in exercised MKOs. Thus, increased cytokine levels, in particular those for TNFα in MKOs, likely contribute to fiber damage by inducing an inflammatory myopathy.

DISCUSSION

Gain-of-function studies *in vitro* and *in vivo* established the importance of PGC-1α in skeletal muscle. Unfortunately, the complex phenotype of the whole body knockout of PGC-1α that included hyperactivity confounded, to a great extent, analysis of skeletal muscle structure and function in these animals. In the skeletal muscle-specific PGC-1α knock-out animal model studied here, we now conclusively show that PGC-1α is required for the maintenance of a normal number of oxidative type I and type IIa muscle fibers. Accordingly, PGC-1α MKO mice are not able to match physical performance of control animals. This was shown for voluntary physical activity, forced isometric muscle endurance in grip strength tests, and dynamic muscle endurance in

treadmill running. In addition to their distinct functions, PGC-1α and PGC-1β share common protein binding partners and the regulation of certain gene programs in skeletal muscle (4, 5). It is thus conceivable that PGC-1β could at least partially compensate for the lack of PGC-1α. However, no compensatory regulation of PGC-1β gene expression in skeletal muscle of MKOs was observed.

A surprising finding was that mice with a specific ablation of PGC-1α in skeletal muscle have increased signs of muscle fiber damage and regeneration. Under basal conditions, this damage does not lead to reduced muscle weight (supplemental Fig. S4*A*). Despite the protection observed in PGC-1α muscle transgenic animals against denervation-induced muscle atrophy, MKOs show no increased propensity for disuse-mediated muscle atrophy (supplemental Fig. S4*A*). Accordingly, expression of atrogenes that control muscle atrophy is not elevated (supplemental Fig. S4*B*). Interestingly, the muscle injury in MKOs is dramatically exacerbated by physical activity. Different factors could contribute to the muscle pathology in MKOs. First, these animals have a reduction in mitochondrial gene expression. Mitochondrial dysfunction is associated with muscle damage in Duchenne muscular dystrophy (26, 27). Second, reactive oxygen species detoxification is crucially regulated by PGC-1α (28) and the levels of a number of reactive oxygen species detoxification genes are reduced in MKOs, including superoxide dismutase 1, superoxide dismutase 2, adenine nucleotide transporter, and glutathione peroxidase 1 (14). Reactive oxygen species cause membrane and protein modifications and have been causally linked to muscle damage (29). In addition, we recently found that PGC-1α regulates the gene program involved in postsynaptic neuromuscular junction plasticity (14). MKOs have a lower number of acetylcholine clusters on muscle fiber membranes (14) and thus might be insufficiently innervated. Finally, systemic inflammation, acute and chronic, is a strong promoter of skeletal muscle wasting. In MKOs, we observed increased levels of circulating cytokines interleukin 6 and TNFα. In particular, the rise in plasma TNFα levels paralleled the dramatic increase in muscle fiber damage post-exercise. TNFα is known to cause inflammatory myopathies in rodent models and human patients (30, 31). Our hypothesis that increased systemic inflammation in MKOs might contribute to the myopathy is supported by other physiological and behavioral abnormalities in these mice. The decrease in body weight and fat mass, reduced physical activity, skeletal muscle damage, increased body temperature and basal metabolic rate, and diminished food intake[4] are compatible with symptoms observed in animal models and human patients suffering from chronic inflammation.

In summary, our findings both confirm data obtained from gain-of-function experimental models and provide novel, surprising insights into the function of PGC-1α in skeletal muscle. The results highlight the central role for PGC-1α to integrate motor neuron input and regulate gene programs involved in oxidative fiber-type determination and muscle fiber endurance. Furthermore, our data show that PGC-1α is important for maintaining skeletal muscle fiber integrity, especially after physical stress. The observation of inflammatory myopathy and overall signs of chronic inflammation in MKOs open novel avenues in our understanding of these devastating muscle diseases and might result in alternative ways of preventing and treating skeletal muscle dysfunctions.

REFERENCES

1. Olson, E. N., and Williams, R. S. (2000) *Cell* **101,** 689–692
2. Hood, D. A. (2001) *J. Appl. Physiol.* **90,** 1137–1157
3. Bassel-Duby, R., and Olson, E. N. (2006) *Annu. Rev. Biochem.* **75,** 19–37
4. Handschin, C., and Spiegelman, B. M. (2006) *Endocr. Rev.* **27,** 728–735
5. Lin, J., Handschin, C., and Spiegelman, B. M. (2005) *Cell Metab.* **1,** 361–370
6. Lin, J., Wu, H., Tarr, P. T., Zhang, C. Y., Wu, Z., Boss, O., Michael, L. F., Puigserver, P., Isotani, E., Olson, E. N., Lowell, B. B., Bassel-Duby, R., and Spiegelman, B. M. (2002) *Nature* **418,** 797–801
7. Czubryt, M. P., McAnally, J., Fishman, G. I., and Olson, E. N. (2003) *Proc. Natl. Acad. Sci. U. S. A.* **100,** 1711–1716
8. Handschin, C., Rhee, J., Lin, J., Tarr, P. T., and Spiegelman, B. M. (2003) *Proc. Natl. Acad. Sci. U. S. A.* **100,** 7111–7116
9. Wu, Z., Puigserver, P., Andersson, U., Zhang, C., Adelmant, G., Mootha, V., Troy, A., Cinti, S., Lowell, B., Scarpulla, R. C., and Spiegelman, B. M. (1999) *Cell* **98,** 115–124
10. Mootha, V. K., Handschin, C., Arlow, D., Xie, X., St. Pierre, J., Sihag, S., Yang, W., Altshuler, D., Puigserver, P., Patterson, N., Willy, P. J., Schulman, I. G., Heyman, R. A., Lander, E. S., and Spiegelman, B. M. (2004) *Proc. Natl. Acad. Sci. U. S. A.* **101,** 6570–6575
11. Schreiber, S. N., Emter, R., Hock, M. B., Knutti, D., Cardenas, J., Podvinec, M., Oakeley, E. J., and Kralli, A. (2004) *Proc. Natl. Acad. Sci. U. S. A.* **101,** 6472–6477
12. Handschin, C., and Mootha, V. K. (2005) *Drug Discov. Today Ther. Strateg.* **2,** 151–156
13. Gleyzer, N., Vercauteren, K., and Scarpulla, R. C. (2005) *Mol. Cell. Biol.* **25,** 1354–1366
14. Handschin, C., Kobayashi, Y. M., Chin, S., Seale, P., Campbell, K. P., and Spiegelman, B. M. (2007) *Genes Dev.* **21,** 770–783
15. Sandri, M., Lin, J., Handschin, C., Yang, W., Arany, Z. P., Lecker, S. H., Goldberg, A. L., and Spiegelman, B. M. (2006) *Proc. Natl. Acad. Sci. U. S. A.* **103,** 16260–16265
16. Lin, J., Wu, P. H., Tarr, P. T., Lindenberg, K. S., St.-Pierre, J., Zhang, C. Y., Mootha, V. K., Jager, S., Vianna, C. R., Reznick, R. M., Cui, L., Manieri, M., Donovan, M. X., Wu, Z., Cooper, M. P., Fan, M. C., Rohas, L. M., Zavacki, A. M., Cinti, S., Shulman, G. I., Lowell, B. B., Krainc, D., and Spiegelman, B. M. (2004) *Cell* **119,** 121–135
17. Arany, Z., He, H., Lin, J., Hoyer, K., Handschin, C., Toka, O., Ahmad, F., Matsui, T., Chin, S., Wu, P. H., Rybkin, I. I., Shelton, J. M., Manieri, M., Cinti, S., Schoen, F. J., Bassel-Duby, R., Rosenzweig, A., Ingwall, J. S., and Spiegelman, B. M. (2005) *Cell Metab.* **1,** 259–271
18. Liu, C., Li, S., Liu, T., Borjigin, J., and Lin, J. D. (2007) *Nature* **447,** 477–481
19. Handschin, C., Lin, J., Rhee, J., Peyer, A. K., Chin, S., Wu, P. H., Meyer, U. A., and Spiegelman, B. M. (2005) *Cell* **122,** 505–515
20. Waters, R. E., Rotevatn, S., Li, P., Annex, B. H., and Yan, Z. (2004) *Am. J. Physiol.* **287,** C1342-C1348
21. Leone, T. C., Lehman, J. J., Finck, B. N., Schaeffer, P. J., Wende, A. R., Boudina, S., Courtois, M., Wozniak, D. F., Sambandam, N., Bernal-Mizrachi, C., Chen, Z., Holloszy, J. O., Medeiros, D. M., Schmidt, R. E., Saffitz, J. E., Abel, E. D., Semenkovich, C. F., and Kelly, D. P. (2005) *PLoS Biol.* **3,** e101
22. Russell, A. P., Feilchenfeldt, J., Schreiber, S., Praz, M., Crettenand, A., Gobelet, C., Meier, C. A., Bell, D. R., Kralli, A., Giacobino, J. P., and Deriaz, O. (2003) *Diabetes* **52,** 2874–2881
23. Seale, P., Sabourin, L. A., Girgis-Gabardo, A., Mansouri, A., Gruss, P., and Rudnicki, M. A. (2000) *Cell* **102,** 777–786
24. Olguin, H. C., Yang, Z., Tapscott, S. J., and Olwin, B. B. (2007) *J. Cell Biol.* **177,** 769–779
25. Dalakas, M. C. (2006) *Nat. Clin. Pract. Rheumatol.* **2,** 219–227
26. Kuznetsov, A. V., Winkler, K., Wiedemann, F. R., von Bossanyi, P., Dietzmann, K., and Kunz, W. S. (1998) *Mol. Cell. Biochem.* **183,** 87–96

27. Timmons, J. A., Larsson, O., Jansson, E., Fischer, H., Gustafsson, T., Greenhaff, P. L., Ridden, J., Rachman, J., Peyrard-Janvid, M., Wahlestedt, C., and Sundberg, C. J. (2005) *FASEB J.* **19,** 750–760
28. St.-Pierre, J., Drori, S., Uldry, M., Silvaggi, J. M., Rhee, J., Jager, S., Handschin, C., Zheng, K., Lin, J., Yang, W., Simon, D. K., Bachoo, R., and Spiegelman, B. M. (2006) *Cell* **127,** 397–408
29. Disatnik, M. H., Dhawan, J., Yu, Y., Beal, M. F., Whirl, M. M., Franco, A. A., and Rando, T. A. (1998) *J. Neurol. Sci.* **161,** 77–84
30. Salomonsson, S., and Lundberg, I. E. (2006) *Autoimmunity* **39,** 177–190
31. Grundtman, C., and Lundberg, I. E. (2006) *Curr. Rheumatol. Rep.* **8,** 188–195

SKELETAL MUSCLE FIBER-TYPE SWITCHING, EXERCISE INTOLERANCE AND MYOPATHY IN PGC-1α MUSCLE-SPECIFIC KNOCKOUT ANIMALS*

Christoph Handschin[1,2], Sherry Chin[1], Ping Li[3], Fenfen Liu[4], Eleftheria Maratos-Flier[4], Nathan K. LeBrasseur[5], Zhen Yan[3], and Bruce M. Spiegelman[1,6]

[1]Dana-Farber Cancer Institute and Department of Cell Biology, Harvard Medical School, Boston, MA 02115, USA
[2]Institute of Physiology and Zurich Center for Integrative Human Physiology (ZIHP), University of Zurich, Winterthurerstrasse 190, CH-8057 Zurich, Switzerland
[3]Department of Medicine, Duke University Medical Center, Durham, NC 27704, USA
[4]Division of Endocrinology, Diabetes and Metabolism, Department of Medicine, Beth Israel Deaconess Medical Center and Harvard Medical School, Boston, MA 02215, USA
[5]Diabetes and Metabolism Unit, Boston University School of Medicine, Boston, MA 02118, USA

Running title: PGC-1α and skeletal muscle function

[6]Correspondence: Bruce M. Spiegelman, Dana-Farber Cancer Institute, Smith Building, One Jimmy Fund Way, Boston, MA 02115, Phone: 617 632 3567, Fax: 617 632 4655, Email: bruce_spiegelman@dfci.harvard.edu

SUPPLEMENTAL FIGURES

Supplemental Fig. S1. Fiber-type switch towards glycolytic fibers in MKOs. The relative number of muscle fibers were quantified by counting type I (red color), type IIa (blue color), type IIx (unstained, black color) and type IIb fibers (green color) in twenty histological sections of gastrocnemius (panel A), plantaris (panel B), tibialis anterior (panel C) and soleus (panel D). *$p<0.05$ between control and MKO animals.

Supplemental Fig. S2. Treadmill running protocol. Control and MKO mice were run on a treadmill with increment increase in speed. Control mice performed significantly better than MKOs.

Supplemental Fig. S3. Increased expression of markers for cell proliferation in PGC-1α MKOs. Relative gene expression from pooled mRNA of the gastrocnemius of 6 mice was analyzed by real-time PCR and normalized to 18S rRNA levels. Abbreviations: P/CAF: p300/CBP-associated factor; GST1: G1 to S phase transition 1; UBE2: ubiquitine-conjugating enzyme E2 variant 2; MAPRE3: microtubule-associated protein RP/EB Family Member 3; APC5: anaphase promoting complex subunit 5; PCNA: proliferating cell nuclear antigen; GADD45: growth arrest and DNA damage-inducible gene b; RBB4: retinoblastoma binding protein 4.

Supplemental Fig. S4. No exacerbation of muscle atrophy by PGC-1α knockout. A, Relative gene expression of cDNA from gastrocnemius muscle and normalized to 18S rRNA levels. Abbreviations: IGF-1, insulin-like growth factor 1; MuRF-1, muscle-specific ring finger protein 1. **B,** Muscle weights from innervated and denervated hind legs. Disuse-mediated muscle atrophy was induced by surgical ablation of the sciatic nerve to one hind leg. Muscle mass was determined 12 days after hind leg denervation. Bars depict mean values and error bars represent standard error. *$p<0.05$ between control and MKO animals.

Supplemental Fig. S1

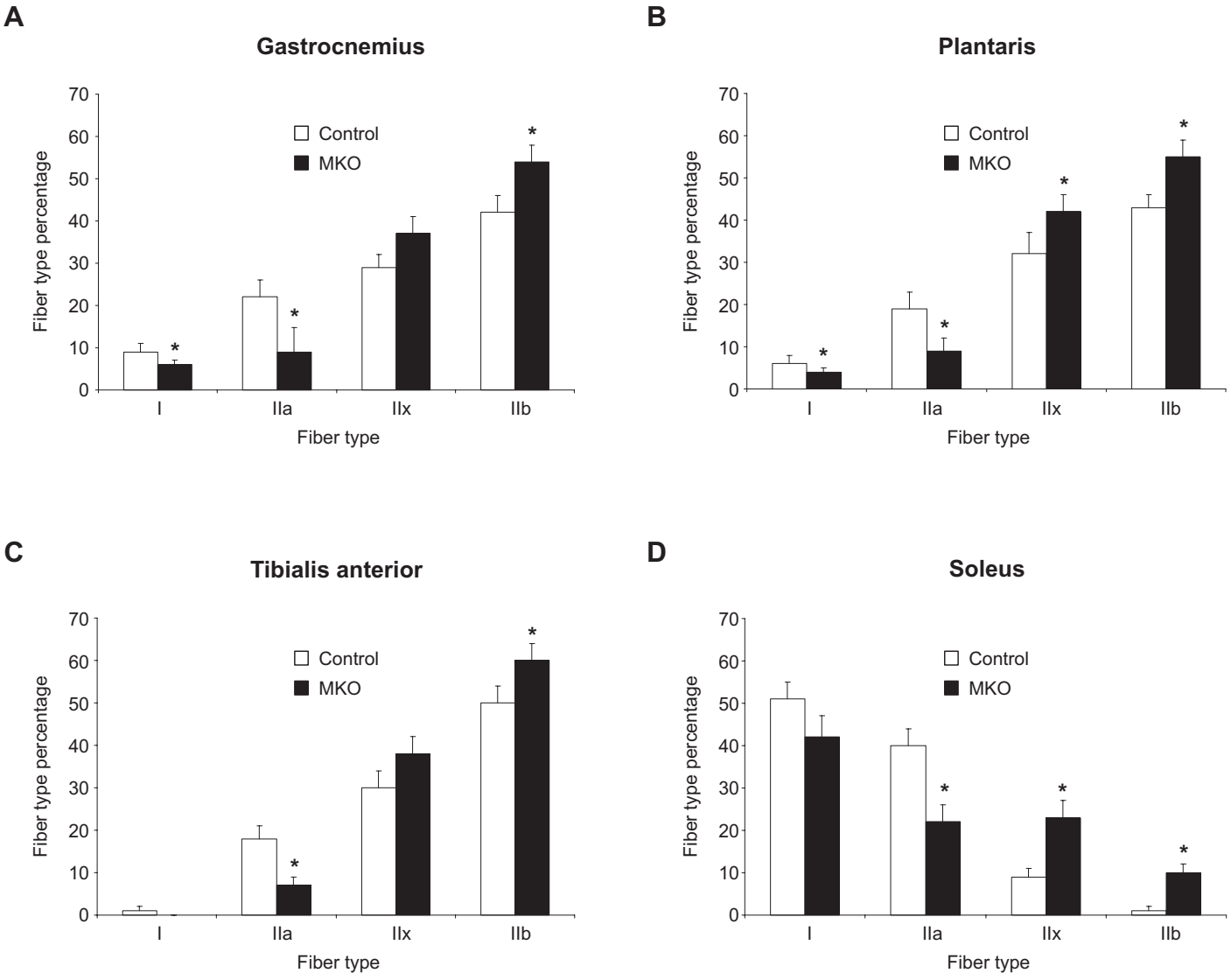

Supplemental Fig. S2

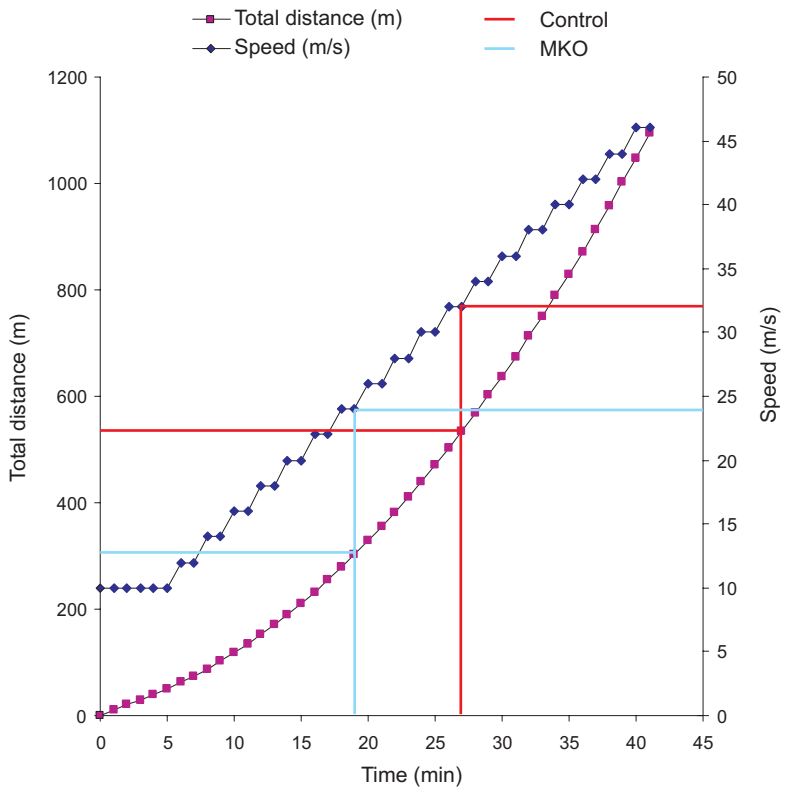

Supplemental Fig. S3

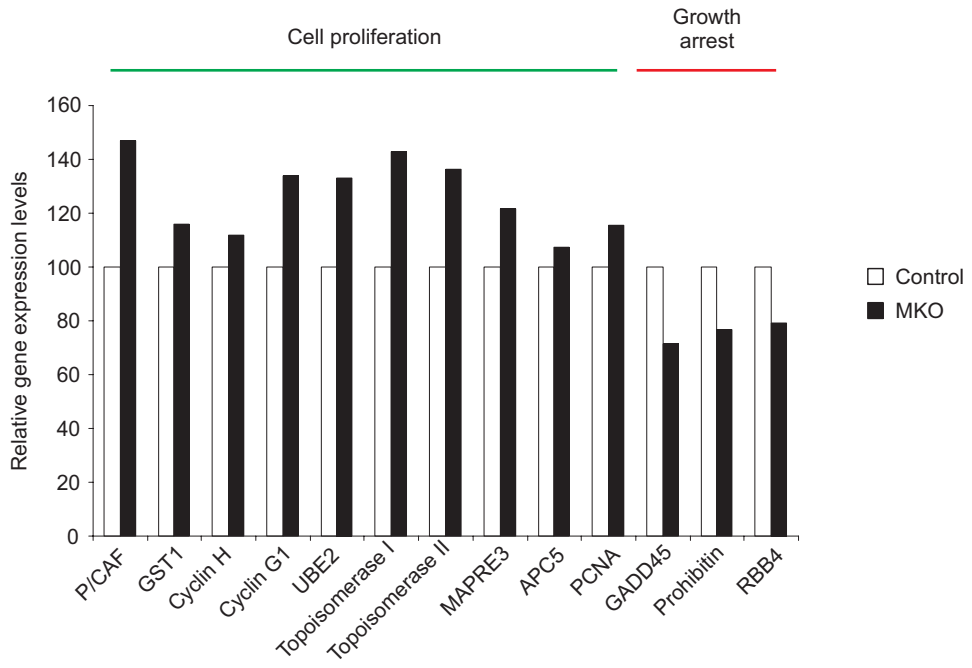

Supplemental Fig. S4

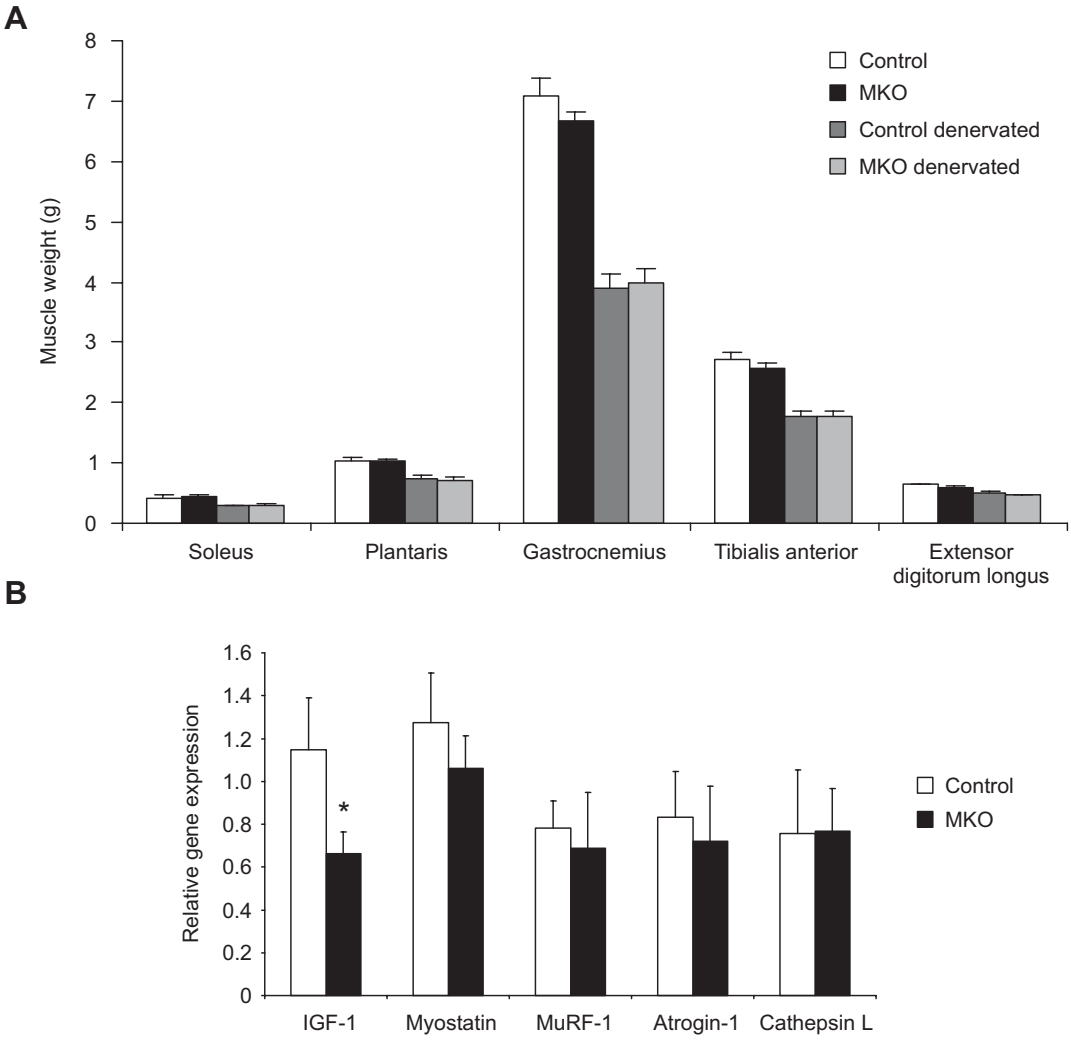

Skeletal Muscle Fiber-type Switching, Exercise Intolerance, and Myopathy in PGC-1 α Muscle-specific Knock-out Animals

Christoph Handschin, Sherry Chin, Ping Li, Fenfen Liu, Eleftheria Maratos-Flier, Nathan K. LeBrasseur, Zhen Yan and Bruce M. Spiegelman

J. Biol. Chem. 2007, 282:30014-30021.
doi: 10.1074/jbc.M704817200 originally published online August 16, 2007
